Nat. Volatiles & Essent. Oils, 2021; 8(4): 14124-14143

NVEO
Natural Volatiles &
Essential Oils

Synthesis, Spectroscopic, Antibacterial, Antifungal, And Toxicity Studies Schiff Base Basing 2-Aminobenzoic Acid Transition Metal Complexes

Abdul Salam Abdul Kareem Abdul Rahman[1] and Rehab Kadhim Raheem alshemary[2*]

[1]Department of chemistry / College of education for pure science| University of Diyala

[2]Department of chemistry / college of Education for Pure Science (Ibn Al-Haitham), University of Baghdad, Baghdad, Iraq

ABSTRACT

The new Co(II), Cu(II), Mn(II), Zn(II), and Ni(II) complexes, including H2DAPB by reacting 2- aminobenzoic acid with 4-amino antipyrine and glyoxylic acid. The new complexes were recognized by diverse spectroscopic methods, and the arrangement of the complexes was assured by Mass spectra and (TGA and DTG) thermal analyses. The in vitro antifungal and antibacterial efficiencies of the compounds were screened versus fungi like C. Albicans, A. niger R. stolonifer, and A. flavus, and bacteria such as S. aureus, E. coli, P. aeruginosa, B. subtilis. All the metal complexes offered powerful antifungal and bacterial efficiencies than the ligand. The linking ability of CT-DNA with the complexes was carried out by photophysical (emission titration /absorption) methods in which an interactive mode of binding was observed. Moreover, outcomes of the DNA-cleavage efficacy propose which the ligand and its metal complexes may cleave CT-DNA at various degrees. Then, the study of interaction for complexes with CT-DNA has been inspected by viscometric and absorption spectral titration determents. Cytotoxicity studies of complexes on (MCF-7) cell line of human breast cancer were screened by EtBr in (MTT) test. Cell viability 50%was given at 25 µg for Cu (II),50 µg for Co(II), 100µg for Mn(II),150µg for Co(II) and 250 µg for Ni(II). The compounds showed significant activity in the biological studies.

KEYWORDS: Schiff base, Structure, DNA targeting, octahedral configuration

INTRODUCTION

Resistance of drugs has been an increasing question in the treatment of contagious diseases reasoned by fungi, bacteria, parasites, and viruses. Infectious diseases like dysentery [1], tuberculosis [2], diarrhoea [3], acute respiratory tract infectious [4] .it is necessary to find out more economical, secure, and active chemotherapeutic factors [6]. Recently years, comprehensive

studies have advanced in the area of coordinate components with a particular signal to their biological efficacies [7]. Recent years have attended a great deal of attention in the preparation and description of transition Schiff base metal coordinates of 4-amino antipyrine [8]. Pyrazolone derivatives and particular 4-amino antipyrine are unique reagents due totheir significance in clinical [9], biological [10], analytical [11], and pharmacologicalpurposes that use to prepare a new kind of chemotherapeutic Schiff bases are presently tempting the interest of biochemists [12]. They have been of considerable significance because of their sensitivity, selectivity synthetic, and flexibility with the metal ions [13]. Hence, in this The paper describes the synthesis and characterization of antifungal and antibacterial sensitive transition metal complexes of N2O2 donor type tetradentate Schiff base formed by condensing 4-amino antipyrine and glyoxylic with 2-aminobenzoic acid.

Synthesis of Ligand 3-(((Z)-4-(((Z)-carboxymethylene)amino)-1,5-dimethyl-2-phenyl-1,2- dihydro-3H-pyrazole-3-ylidene)amino)benzoic acid -: A mixture of 2-aminobenzoic acid (0.11g 9.9 mmol), dissolved 10 ml in ethanol and amine compound of (4-amino antipyrine) (0.203 g, 9.9 mmol) dissolved in 10 ml ethanol was refluxed on the water bath for six h under stirring. On cooling to room temperature, was obtained. The crystal was filtered and washed with ethanol; upon completion of the reaction, the product was crystallized in acetone and dried at ambient temperature. Then a solution of Ligand (Z)-2-((4-amino-1,5-dimethyl-2-phenyl- 1,2-dihydro-3H-pyrazole-3-ylidene)amino)benzoic acid (0.319g, 9.9 mmol) in (20 ml) ethanol, and a few drop of (HBr 48%), was desiccated to (0.074 g, 10 mmol) a (Glyoxylic acid) solution of in (10 ml) ethanol. The solution was refluxed with stirring for (6 hr). The resulting was a brown solution allowed to cool and desiccated at room temperature. After that, clean with solvent and re-crystallization to the residue with H2O/methanol to result in a dark orange precipitate (24 hr).

Synthesis of its complexes

The following overall procedure was selected for the preparation of its complexes. To the ligand DAPB (0.01 M) dissolved in (15 ml) ethanol of the competent divalent metal chloride [(0.01M) Co(II), Mn(II), Zn(II), Ni(II), and Cu(II)] was added slowly. Each solution was patronized with10% KOH solution to regulate the pH to 7–8 range, and the resultant mixture was heated underreflux for three h on a hot mantle. The bright-coloured metal complexes thus separated were filtered, washed successively with small amounts of distilled water, methanol, and petroleum ether, and dried in a vacuum. The purity of the complexes was tested by thin-layer chromatography using different solvent mixtures.

In vitro assay for anti-cancer activity (MTT assay)

Cells (1 × 10^5/well) were coated in 24-well sheets at 37 °C and incubated with 5% CO_2 condition. After the cell reaches the confluence, the various concentrations of the samples were added and incubated for 24 hours. After incubation, the sample was removed from the well and washed with phosphate-buffered saline (pH 7.4) or MEM without serum. 100 µl/well (5 mg/ml) of 0.5% 3-(4,5-dimethyl-2-thiazolyl)-2,5-diphenyl-tetrazolium bromide (MTT) was added and incubated for 4 hours. After incubation, 1 ml of DMSO was added to all the wells. The absorbance at 570 nm was measured with UV-Spectrophotometer using DMSO as the blank. The concentration desired, and determinations were completed for an (IC50) 50% inhibitions were measured graphically. The % cell viability was determined utilizing the following formula:

% cell viability = A570 of treated cells/A570 of control cells × 100

Graphs are plotted to employ the concentration of the sample on the X-axis and the % of Cell Viability on the Y-axis. Sample hegemony and cell hegemony are contained in each screening to liken the whole-cell viability in cytotoxicity and anti-cancer efficiency assessments.

2.5.1. Absorption Titration

The titration of electronic absorption spectral of Cu, Ni, Co Mn, and Zn complexes with C.T.- DNA was completed in Tris-HCl buffer (pH = 7.2).

2.5.2. Competitive Binding

The competitive binding of Cu, Ni, Co, Mn, and Zn complexes with EtBr link DNA in Tris- a buffer of HCl/NaCl (pH 7.2) was inspected by utilizing spectroscopy of fluorescence.

2.5.3. Viscosity

In command to estimate the interaction of hydrodynamic between ligand and particles of C.T.-DNA stabilized metal, and the viscosity instruments were completed at room temperature utilizing Ostwald's viscometer maintained. Data were showed as $(\eta/\eta 0)^{1/3}$ vs [Complex]/[DNA], where ηand η0 is the viscosity of DNA in the absence and presence of the complexes. Viscosity data were determined from the noticed flow time of DNA,including solutions corrected for buffer alone η = (t − t0) (Tris-HCl) (t0).

Gel Electrophoresis

The gel electrophoresis tests were completed by incubation for 2 h at 35°C as follows: 50 µM H_2O_2, 30 µM CT DNA, each Complex (50 µM) in Tris-HCl buffer (50 mM) (Ph=7.2). The specimens were

electrophoresed pH 7.2 employing 14 8 EDTA- tris-acetic acid buffer at 50 V on 1% agarose gel for 2 h. The gel was stained employing one μg/cm^3 E.B. and photographed under the light of U.V. after electro-15 phoresis.

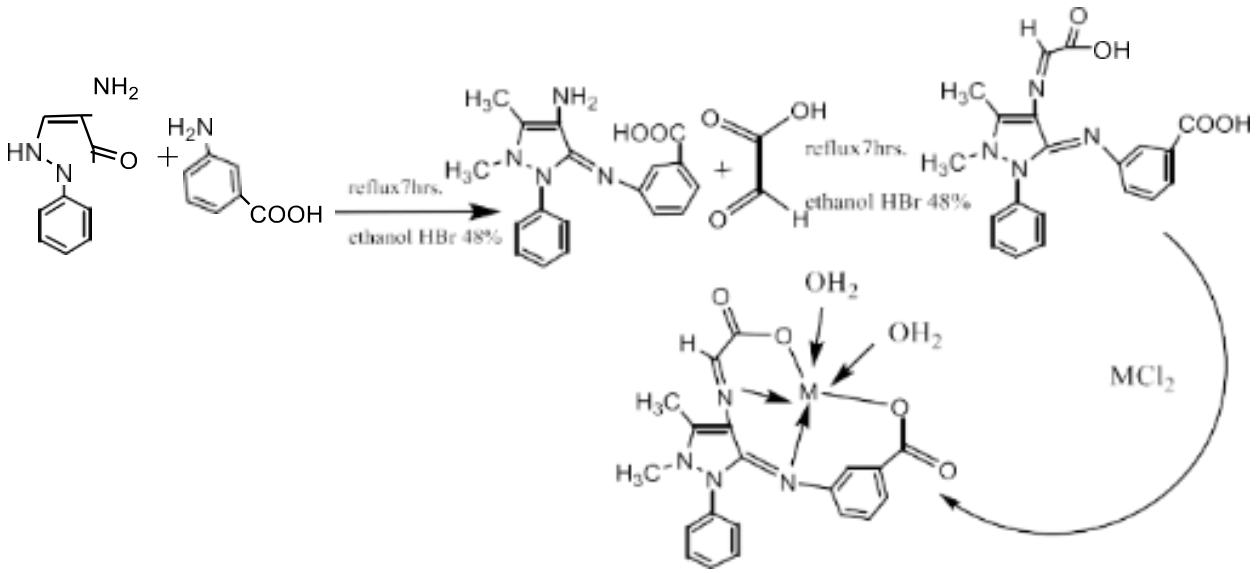

M=Ni(II),Co(II), Cu(II),Mn(II) and Zn(II)

Table (1): Some physical properties of prepared ligand (DAPB) and its complexes

Empirical formula	Formula Mwt	Mwt g/mol	Color	Dec. ° C	Yield %	Elemental Analysis %Found(calculated)			
						C	**H**	**N**	**M**
H_2DAPB	C20H18N4O4	378.39	Dark orange	210	58	62.87 (63.49)	4.17 (4.80)	14.21 (14.81)	-
[Co(DAPB)$(H_2O)_2$].H_2O	C20H20CoN4O6	471.34	Brown	300	57	67.27 (50.97)	67.27 (4.28)	67.27 (11.89)	67.27 (12.50)
[Ni(DAPB)$(H_2O)_2$].H_2O	C20H20N4NiO6	471.10	Dark green	282	79	55.30 (50.99)	55.30 (4.28)	55.30 (11.89)	55.30 (12.4)

[Cu(DAPB)(H_2O)$_2$]	C20H20CuN4O6	475.95	Dark brown	> 320	60	67.27 (50.47)	55.27 (4.24)	55.27 (11.77)	55.27 (13.35)
[Mn(DAPB)(H_2O)$_2$]	C20H20MnN4O6	467.34	Pale brown	> 320	78	55.09 (51.40)	55.09 (4.31)	55.09 (11.99)	55.09 (11.76
[Zn(DAPB)(H_2O)$_2$]	C20H20N4O6Zn	477.78	Pale brown	> 320	71	55.87 (50.28)	55.87 (4.22)	55.87 (11.73)	55.87 (13.68)

Table (3): I.R. spectral data of the ligand and its metal complexes

Comp.	υ(O.H.) υ(O.H.)water	υ(C.H.)	υ(C=O) carboxylic	υ(C=N) imine	υ (C=C)	υasy. (COO^-)	$υ_{sy.}$ (COO^-)	$υ_{asy.}$-$υ_{sy.}$ (COO^-)	υ(M-N) υ (M-O)
(DAPB)	3245 3276	3063 2976	1686	1657 1550	1569	-	-	-	----
[Co(DAPB)(H2O)2].H2O	3411	3074 2967	-	1621 1520	1566	1505	1404	101	615 471
[Ni(DAPB)(H2O)2].H2O	3428	3084 2971	-	1632 1530	1564	1495	1383	112	596 467
[Cu(DAPB)(H2O)2]	3432	3060 2957	-	1625 1524	1562	1491	1372	119	614 461
[Mn(DAPB)(H2O)2]	3415	3084 2981	-	1631 1528	1568	1487	1377	110	608 469
[Zn(DAPB)(H2O)2]	3420	3059 2975	-	1634 1526	1565	1490	1379	111	604 463

Table (4): Electronic spectral data of the ligand and its metal complexes

Compounds	**µeff**	**ʌmohm**	**λ nm**	**ᵡ cm^{-1}**	**Ɛmax (mola**	**Transition**	geometry

		.cm^2 mol ar$^-$ 1			**r$^-$1 .cm^{-1})**		
DAPB	-	-	259	38610	2399	(π → π*)	
			341	29325	150	(n→ π*)	
[Co(DAPB)(H$_2$O)$_2$].2H$_2$O	3.9	72	260	38461	2399	L.F	Octahedral
			341	29325	150	CT	
			418	23923	100	(^{4}T1g → ^{4}T1g(P))	
			741	13495	4	(^{4}T$_1$g → ^{4}A$_2$g)	
[Ni(DAPB)(H$_2$O)$_2$] H$_2$O	2.2	77	248	41152	2449	L.F	Octahedral
			346	28901	175	CT	
			389	28169	110	(^{3}A2g→^{3}T1g(P))	
			482	21052	10	(^{3}A$_2$g→^{3}T$_1$g)	
			841	12180	4	(^{3}A$_2$g→^{3}T$_2$g)	
[Cu(DAPB)(H$_2$O)$_2$]	3.4	86	250	40000	2467	L.F	Octahedral
			343	29154	167	CT	
			395	25316	121	(^{2}B$_1$g→^{2}Eg)	
			789	1291	32	(^{2}B$_1$g→^{2}A$_2$g)	

				9			

[Mn(DAPB)(H_2O)$_2$]	5.40	79	252	41493	2418	L.F	Octahedral
			348	28169	189	CT	
			390	25641	133	($^6A_1g \rightarrow {}^4A_1g$, ^4Eg (G))	
			458	23095	987	($^6A1g \rightarrow {}^4T2$ g(G))	
			653	16393	41	($^6A1g \rightarrow {}^4T1$ g(G))	
[Zn(DAPB)(H_2O)$_2$]	-	82	247	40485	2289	L.F	Octahedral
			355	28169	320	CT	
			401	24937	250	C. T	

3.1. NMR spectra

^{1}H NMR spectrum for [DAPB)] in DMSO-d6 displayed signal at chemical shift (δH = 1.85 ppm, 3H, s) referred to the proton of the **C<u>H</u>$_3$-C** moiety,(δH = 2.47ppm, 3H, s) referred to the proton of the**C<u>H</u>$_3$-C=** moiety and (δH = 8.80ppm, 1H, s) referred to the proton of the **C<u>H</u>=N** moiety. The resonances at chemical shift (δH = 7.08-8.38ppm, 13H, m), (Ar–H), are assignable to protons of the aromatic ring. The signal at (δH = 12.31ppm, 1H) and (δH = 12.81 ppm, 1H) are assignable to protons of (COO<u>H</u>) carboxylic group of glyoxylic acid and (COO<u>H</u>) carboxylic group of benzoic acid, respectively. The spectrum displayed chemical shifts at (δH = 2.50 ppm) referred to as the DMSO solvent. The results are summarized in table (2).

The ^{13}CNMR spectrum of (H.L.) in DMSO-d6 showed a signal at chemical shift (δ=4.34 ppm) attributed to the carbon atom of the **<u>C</u>H$_3$-C=**group, a signal at chemical shift at (δ=30.41 ppm) assigned to the carbon atom of the **<u>C</u>H$_3$-C-**group. The chemical shifts at(δ=168.35 ppm)and(δ=172.35ppm) attributed

to the carboxylic carbon atom **C**OOH of glyoxylic acid and the carboxyliccarbon atom **C**OOH of benzoic acid respectively, while the chemical shifts at (δ= 150.17and 155.07ppm) are assigned for imine carbon atoms (-**C**=N-) respectively. The chemical shifts at(110.16 ppm) assigned to carbon atoms of the (**C**-N) group. At last, the chemical shifts (δ=124.28-
132.04 ppm) refer to **C**=C carbon atoms. The results are listed in Table (4).

3.2. I.R. spectra

The infrared spectrum of the ligand was showed abroad hesitancies at (3245 and 3276 cm^{-1}), which were due to (-O.H.) carboxyl groups [14]. The υ(O-H) bands are absent in the I.R. spectrum of the complexes due to that the carboxyl O.H. protons were lost upon complexation [15]. Another board band showed (3411-3432cm^{-1}) in the spectrum of complexes. The bonds in the ligand spectrum were noticed at (1657, 1550) cm^{-1}in the spectrum of Schiff base ligand due to υ(C=N) imines linkage were moved towards lower hesitancies in all the complexes. Other sharp bands showed (1686cm^{-1}) carboxyl groups. These hesitancies were moving to greater and fewer hesitations(1634-1621cm^{-1}) and (1530-1520cm^{-1}) results in all the complexes, Δυ = (υasym. (COO^-)-υsym. (COO^-
)) in range (101-111) in the spectra of the chelate complexes signalizes the participation of deprotonated carboxylic groups (COOH) in chelation and bonding of metal ions through oxygen atoms of carboxyl groups. Furthermore, evidence of the chelation to N and O was supplied by the manifestation of the bands υ(M-N) and υ(M-O) in the (615-596 cm^{-1}) and(471-461cm^{-1}) region in the spectra of the complexes [16]. The results are listed in Table (4).

3.3. Electronic spectra

The Complex's spectra were registered in DMSO solution. All the synthesized complexes presented the elevated energy absorption band in the zone (38461- 41493) cm^{-1} and (28169-29325) $cm^{-1.}$ These transferences may be indicated to the ligand field and charge transfer bands.

The U.V.-Vis spectrum of Co(II) complex presented the two d-d transferences bands in the region23923 and 13495 cm^{-1} which are assigned to ($^4T1g \rightarrow {}^4T1g(P)$) and ($^4T1g \rightarrow {}^4A2g$) transitions, respectively. The transitions support an octahedral arrangement of the Complex, which is also supported by its magnetic sensitivity data (3.9lB).

The U.V.-Vis spectrum of Ni(II) complex presented three d–d bands at 28169, 21052, and 12180 cm^{-1}. These identities to ($^3A2g \rightarrow {}^3T1g(P)$), ($^3A2g \rightarrow {}^3T1g$), and ($^3A2g \rightarrow {}^3T2g$) transferences, respectively, being diagnosis of an octahedral arrangement. This arrangement is moreover confirmed by its magnetic sensitivity data (2.2lB).

The Cu(II) complex spectrum of offered the two (d-d) transition bands in the areas 25316cm^{-1} and 12919$cm^{-1,}$ which are due to ($^2B1g \rightarrow {}^2Eg$) and ($^2B1g \rightarrow {}^2A2g$) transitions, respectively. These d–d band transition bands robustly support an octahedral arrangement around the metal ion.

The U.V.-Vis spectrum of Mn(II) complex presented the two d-d transition

bands in the region 25641 cm^{-1}, 23095 cm^{-1} and 16393cm^{-1} which are assigned ($^6A1g \rightarrow {}^4A1g, {}^4Eg(G)$),($^6A1g \rightarrow {}^4T2g(G)$) and ($^6A1g \rightarrow {}^4T1g(G)$)transitions, respectively. The transitions support the octahedral arrangement of the Complex, which is also supported by its magnetic sensitivity data (5.40lB). The Complex of Zn(II) is diamagnetic. Conformity to the experimental form, an octahedral arrangement is suggested for this Complex. The results are listed in Table(5).

3.4. Molar conductance of metal complexes

In DMSO solutions of the complexes, conductance samples were recorded for 72-86 ohm.cm^2 $molar^{-1}$. Table 3 summarizes them as non-electrolytes.

3.5. Mass spectra

Mass spectra fit out a necessary guide for illustrating the composition of components. The mass spectra of the Schiff base were determined and applied to liken their stoichiometry installation. The ligand exhibited a molecular ion peak at m/z 378.19 correspondings to equivalent to its molecular weight $[C20H18N4O4]^+$ ion. Also, the spectrum showed the fragments at m/z 200, 122, 121, 93, 76,63 59 and 45 corresponding to $[C11H12N4]^+$, $[C7H5O2]^+$, $[C5H8N4]^+$, [C2H4O2], $[C9H10O2]^+$, $[C6H5]^+$ $[C2H3O2]^+$ and$[COOH]^+$ respectively**.**

3.6. Thermal analyses (TGA and DTG)

The weight lack for one coordinate was determined within the coinciding temperature reigns. The TGA detour of (H2DAPB) displays a 1st appreciated at 30-300 °C mass lack of 48.87%(calked: 47.98%), which may be due to the releasing of CH4 and C6H6 as gases. In the $2^{nd}$and 3^{rd} stapes in the range 400-900 °C, the ligand forfeits the residual portion with an evaluated mass lack of 51.65% (calced: 52.33%) with an entire dismantling as NO, NO2, CO, CO2, etc. gases. The T.G. degradation of complexes was calculated by T.G. analysis from surrounding temperature to 900 °C. The values from the T.G. analysis specified which the dismantling of the complexes produces in 4 or 5 stages. The removal of water from these compounds may be done in one or two steps. Between 20 and 110 °C, all complexes lost hydration water, and beyond 180 °C, the chelated water molecule was lacking. For all complexes, the breakdown was complete at 650 °C. The TGA of the Co(II) coordinate offers three dismantling stages within the

temperaturereign of 30-650 °C.The 1st stage of dismantling in reign 25-500 °C.The berk of hydrated H2O

Molecules were inspected from the exothermic peak around 40-300°C temperature; subsequently, the forming of CoO has remained above 650 °C.

Cu(II) complex undergoes 1st stage of decomposition in the range 60-700 °C, with an estimated mass loss of 14.23% (calcd: 14.68%). This mass loss corresponds to the pyrolysis of the (2nd and3rd) steps include the lack of ligand molecules, leaving CuO a residue. The inclusive weight lack values to 65.22% (calcd: 65.65%), and 21.69% (calcd: 21.05%) for the Cu(II) chelate with ligand, respectively.

Furthermore, The TGA curves of the Ni(II)- coordinate display three steps of dismantling in the reign of 25-620 °C. The 1st stage, at 25-250 °C, coincides with the lack of water molecules of hydration; in the 2nd stage, the chelated water molecule was lack. However, the following (3rd and 4th) steps include the lack of ligand molecules, loss of organic moiety, NiO. The inclusive weight lack values to 65.37% (calcd: 65.89%) and 20.35% (calcd: 20.05) for the Ni(II) chelate with ligand, respectively. For the Mn(II) coordinate, the first step is in the temperature range 60– 98°C (mass loss = 14.03%; calcd for 2H2O (14.31%), which may account for the lack of water molecules of hydration. The mass lacks the existing dismantling stages amount to 21.45% (calcd: 21.25%) and coincide with the elimination of H2O, 1/2 O2, DAPB molecules, leaving 1/2 MnO as a residue. The overall weight loss amounts to 14.36% ((calcd: 14.73%),64.11% (calcd:64.49%), 21.71% (calcd: 21.61%) for the Zn(II)chelates with DAPB ligand, respectively.

Table 4: Thermal (TGA/DTG) analysis of ligand (H_2DAPB) and its complexes.

Complex	Temperature range t (C)	% weight loss Obs. (calcd)	DTA peak t (C)	Process
(H2DAPB)	30-300 , 400-900	48.05(47.23), 52.33(51.65)	80,210, 320,460	CH4(g) , C6H6(g) NO(g) , NO2(g) , CO(g) , CO2(g)
[Co(DAPB)(H2O)2].2H2O	60–98,153–266, 360–560, >560	14.63 (13.98), 65.56(63.78), 20.56(20.11)	97,200 , ,370, 520, 615	2H2O(coord), 1/2 O2 ,H2O(lattice), loss of organic moiety, CoO
[Cu(DAPB)(H2O) 2]	60-165 286-560–>610	14.23(14.68), 65.22(65.65), 21.69(21.05)	195,240, 325, 470, 580	2H2O(coord), , loss of organic moiety, CuO

[Ni(DAPB)(H2O)2].H2 O	25–125, 190-250 ,340–510, >600	14.45(14.87), 65.37(65.89), 20.35(20.05)	70, 230, 380, 520, 620	2H2O(coord), H2O(lattice), loss of organic moiety, NiO
[Mn(DAPB)(H2O)2]	60–98,153–266, >559	14.03(14.31), 64.23(64.61), 21.45(21.25)	197,370,, 615	2H2O(coord),H2O(lattice), loss of organic moiety, MnO
[Zn(DAPB)(H2O)2]	150–260, 350–590, >590	14.36(14.73), 64.11(64.49), 21.71(21.61)	160, 540, 615	2H2O(coord),loss of organic moiety, ZnO

3.7. Biological l activity

Dose relies on antifungal and antibacterial researches of the complexes against four fungi (Fig. 8(b))and four bacteria (Fig. 8(a)) displays which potential antifungal and antibacterial impact. Clearance of zones in range (14-27)mm for A. niger, A. flavus, R. stolonifer, and C. Albicans. respectively for the complexes. Clearance of zones in range (2-18)mm for S. aureus , P. aeruginosa, B. subtilis, E. coli, respectively for the complexes. Results show that the activity of the complexes with fungi and bacteria when likened to standard amphotericin for fungi and standard streptomycin for bacteria and in metals

The Complexes were modest, and the effectiveness of the complexes was somewhat greater than the (DAPB). Antifungal efficacy of the complexes versus fungi results suggests that the zone of inhibitory activity of (DAPB)is equal to the standard drug amphotericin.).Nevertheless, the antibacterial efficacy of the complexes versus bacteria shows that the complexes have higher activity than standard streptomycin**.** These data are shown in table 7.

Table 5: In vitro antimicrobial and antifungal activity of the ligand and its complexes

Compounds	Bacteria				Organism			
	E. coli	**S. aurous**	**B. subtilis**	**P. aeruginosa**	**A. niger**	**A. flavus**	**R. stolonifer**	**C. albicans**
control	1	1	2	2	8	7	7	5
DAPB	2	3	4	5	15	14	17	16
$[Co(DAPB)(H_2O)_2]$].$2H_2O$	7	10	11	10	20	23	26	22
$[Cu(DAPB)(H_2O)_2]$	9	12	16	14	25	26	27	24
$[Ni(DAPB)(H_2O)_2].H_2O$	13	15	15	13	28	23	21	26
$[Mn(DAPB)(H_2O)_2]$	15	17	16	14	26	28	23	25
$[Zn(DAPB)(H_2O)_2]$	12	14	14	18	24	26	26	27

3.8. Cytotoxicity Effect on Cancer Cell Line (MCF-7)

Efficacy of anti-cancer for the complexes & DAPB ligand with cell line of cancer MCF-7was inspected by MTT examination. Cell of cancer MCF-7 was remedied with the complexes and DAPB ligand the % cell viability at 24 h post-exposure (0– 250 µg/mL) was specified Table 8. From the notice, the % of the cell viability Cu, Ni, Mn, Zn, Cocomplexes & DAPB ligand was increased with the accretion of concentration. Cell 50% ,the ability was obtained at 25 µg for Cu(II)complex,50 µg forCo(II)complex100µg for Mn((II)complex , 150µg for Co(II)complex and 250 µg for Ni (II)complex. This result shows which Cu((II)complex have more cytotoxicity by cell line MCF7 cancer than other complexes. Moreover, realizations are necessary to evidence the anti-cancer activity of Cu(II) in the future.

3.9. DNA Binding

Absorption Spectral Titration

The DNA concentration in various additions from (10-100)µL to DAPB steadied metal, the absorption intensity band at 252, 261, and 287 nm for Cu, 246, 264, and 290 nm for Ni 250, 260, and 288 nmfor Co, 244, 258 and 291 nm for Mn and 248, 263 and 294 nm for Zn reduce and transferred to more wave length which proposes the hypochromism with slight red transfer. The previous notices evidenced which DAPB stabilized metals reacted with CT-DNA through hydrophobic interaction attributed to the existence of hydrophobic groups. The harmonic lowering in intensity

of the absorption band of the complexes that (Kb) constant of the intrinsic binding were determined by utilizing the equation

[DNA]/(εa − εf) = [DNA]/(εa − εf) + 1/Kb (εb − εf)

where, [DNA] is the DNA concentration in pairs of base, The Kb data ofCu(II) , Co (II), Ni(II) Zn((II), and Mn(II) complexes were 6.21× 10^4 , 6.19× 10^4 , 6.37× 10^4 6.11× 10^4 and 6.05 ×

10^4 respectively, εf coincides to the coefficient of extinction for the Complex in its free shape and εb indicates to the coefficient of extinction for the Complex in its bound shape εa is the coefficient of apparent extinction got by calculating A_{obs}/[Complex]. Amongst [Cu(DAPB)(H_2O)2] have more binding affinity than, the complexes when links with CT-DNA as appeared Fig.7(a).

3.3.2. Competitive linking

The interaction conduct of interacting the complexes with CT-DNA was moreover assured by titration of fluorescence spectral. From competitive binding (EtBr) ethidium bromide is interchange from EtBr link-DNA by the addendum of 2ndary molecule. This experience was completed by EtBr link DNA with varying concentration of Cu(II) , Co(II), Ni(II), Zn(II), Mn(II)and

[Zn(DAPB)(H_2O)2] in (5 mM /50 mM) buffer of Tris-HCl (pH = 7.0) display in Fig. 7(a). These outcomes show that the growth in the concentration of DPMM-CuNPs & DPMMNiNPs(secondary molecule) could replace the EtBr in EtBr link DNA that assured the competitive binding takes place. Corresponding to the equation of the Stern-Volmer,

I/I0 = 1 + Ksv [Q]

, [Q] is the quencher concentration, I0 and I are the absence and presence of quencher fluorescence intensities, Ksv is the constant of Stern-Volmer quenching. Ksv data of interacting Co (II), Ni (II) , Mn(II) and Zn(II) are 5.43 × 10^3 ,4.74 × 10^3 ,3.36× 10^3, 3.36× 10^3,2.57× 10^3 and 1.08 ×

10^3 respectively. These notices propose that the Cu(II) particles are highly interacting other metal particles with CT-DNA.

Viscosity

The flow of viscous rose as the concentration of interacting complexes to CT-DNA grew during the viscometric instrument. In Fig. 7(a)bar diagram was drawn between relative specific viscosity (η/ η 0) and 1/R, where η and $η^0$ represent the specific viscosity of DNA in the presence and absence of interaction complexes, and 1/R = [Complex]/[DNA] (b). Cu(II) has a higher affinity for DNA than complexes, according to the graph.

Table (6): % of Cell viability of the compounds with MCF7 cancer cell line

% of Cell viability					Concentration (µg/mL)
100	50	25	12.5	5	Compounds
100	100	100	100	10.0	Control
48.2	29.7	31.5	31.8	47.3	(DAPB)
75.7	34.5	42.8	50.8	13.7	[Co(DAPB)(H2O)2].2H2O
52.2	35.1	35.3	50.8	12.7	[Cu(DAPB)(H2O)2]
77.8	33.9	36.5	58.5	17.2	[Ni(DAPB)(H2O)2].H2O
59.3	.34.4	36.1	58.7	17.2	[Cu(DAPB)(H2O)2]
85.7	51.9	60.4	74.8	23.1	[Mn(DAPB)(H2O)2].H2O
61.5	36.7	34.4	39.7	9	[Zn(DAPB)(H2O)2]

Fig.1. a) Titration of CT-DNA complexes via electronic absorption spectroscopy b) Influence of complex viscosity on C.T. -.DNA viscosity

Figure 2: Bioactive compounds: Inhibition zone in mm against various bacteria (a) and fungi (b); in vitro cytotoxicity % versus Mcf-7 cells (c).

$$[DNA]/(\varepsilon a - \varepsilon f) = [DNA]/(\varepsilon a - \varepsilon f) + 1/Kb\ (\varepsilon b - \varepsilon f)$$

where, The Kb data of Cu(II), Co(II), Ni(II), Zn(II), and Mn(II) were 6.32×10^4, 5.54×10^4,4.68×10^4, $3.72\times10^{4,}$ and $6.14\times10^{4,}$ respectively. [DNA] represents the concentration of DNA in base pairs. εa is the optical extinction coefficient obtained by dividing Aobs/[Complex]. ε_b corresponds to the Complex's extinction coefficient in its linking shape. In contrast, ε_f corresponds to the Complex's extinction coefficient in its free form. When interacting with CT-DNA, no compound has a higher binding affinity than (DAPB).

N.A. cleavage studies

All of the complexes converted supercoiled DNA (Form-I) into open circular DNA (FormII). The typical DNA cleavage procedures were carried out in an overall volume of (10 L µL) that included 20 mM Tris-HCl buffer (pH 7.2), 500 µM, CN-DNA, and metal complexes (0.0001 M). The processes were carried out

at 32°C for 120 min. A gel loading buffer containing bromophenol blue as a dye was added. It was immediately loaded on a 1% agarose eight gel for gel electrophoresis at 50 V. The gels were stained with ethidium bromide ($0.1mL^{-1}$) before being photographed using a U.V. transilluminator.

The active DNA-linking capacity of the complexes is attributed to their higher cleavage efficiency compared to the control.Dominance experiences utilizing DNA single cannot display any splitof CT-DNA Even after a longer period of detection time. This consequence detected which the split of DNA in systems of the complexes could be assigned to the DNAsplit. The other complexes displayed the same electrophoretic conduct and split efficacy againstCT-DNA. The findings show that metal complexes play a significant role in the CT-DNA split reaction. The oxidative DNA split by singlet is likely caused by guanine nuclease oxidation.

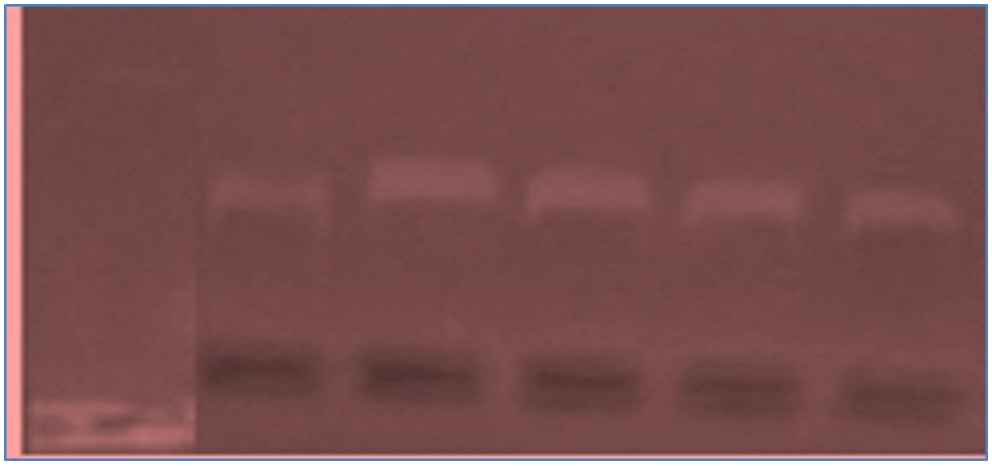

Fig. 3. variations in pattern of the agarose gel electrophoretic for CT- DNA contained by H_2O_2 and all complexes. Lane 1, DNA alone; lane 2, DNA + Co(II)complex; lane 3, DNA + Cu(II); complex; lane 4, DNA + Ni(II) complex; lane 5, DNA + Mn(II) complex; lane 6, DNA + Zn(II) complex .

4. Conclusions

In the actual research, our pains were to composition and described the new Schiff base and its complexes. The Schiff base was derived from 4-amino antipyrine, glyoxylic acid, and 2- aminobenzoic acid.

The Antibacterial and antifungal studies revealed that all of the newly prepared complexes displayed efficiency in a broad spectrum of fungi such as A. flavus, R. stolonifera, A. niger, C. Albicans and bacteria such as E. coli, S. aureus, B. subtilis, P. aeruginosa with the presence of O.H.functional groups on DNA might be effectively cleaved by an electrochemically contained way. All the complexes have more efficacy than the control CT-DNA. The complexes have more activity than the other complexes and the

control. And reproductive efficiency of the complexes with a cell line of cancer MCF-7 then display which Cu(II) complex have more activity than other complexes

References

1. Stacy, A.E., Palanimuthu, D. Bernhardt, P.V , Kalinowski,. D.S., Jansson, P.J., Richardson, D.R., Zinc(II)–thiosemicarbazone complexes are localized to the lysosomal compartment where they transmetallate with copper ions to induce cytotoxicity, J. Med. Chem. 2016; 59, 4965–4984.
2. Raman, N., Raja, S.J. and Salkthivel, A. Transition Metal Complexes with Schiff-Base Ligands: 4-Aminoantipyrine Based Derivatives—A Review, Journal of Coordination Chemistry 2009;**62**,691-709.http://dx.doi.org/10.1080/009589708 02326179
3. Rosu, T., Pahontu, E., Maxim, C., Georgescu, R., Stanica, N. and Gulea, A. Some New Cu(II) Complexes Containing an on Donor Schiff Base: Synthesis, Characterization and Antibacterial Activity, Polyhedron 2011;**30**, 154-162. http://dx.doi.org/10.1016/j.poly. 2010.10.001
4. Mohamed, G.G., Omar, M.M. and Ibrahim, A.A. Biological Activity Studies on Metal Complexes of Novel Tridentate Schiff Base Ligand. Spectroscopic and Thermal Characterization, European Journal of Medicinal Chemistry 2009; **44**, 4801-4812. http://dx.doi.org/10.1016/j.ejmech.2009.07.028
5. Elemike, E.E. Oviawe AP. and Otuokere, I.E., Potentiation of the Antimicrobial Activity of 4-Benzylimino-2,3- Dimethyl-1-phenylpyrazal-5-one by Metal Chelation, Research Journal of Chemical Sciences 2011; 1, 6-11.
6. W.J. Lian, X.T. Wang, C.Z. Xie, H. Tian, X.Q. Song, H.T. Pan, X. Qiao, J.Y. Xu, Mixed- ligand copper(II) Schiff base complexes: the role of the co-ligand in DNA binding, DNA cleavage, protein binding and cytotoxicity, Dalton Trans. 2016; 45 9073–9087.
7. Acheson, R.M. Introduction to Heterocyclic Compounds. 4th Edition, Wiley, New York ; 2009.
8. Gopalakrishman, S. and Joseph, J., Antifungal Activities of Copper (II) with Bio sensitive Macrocyclic Schiff Base Ligands Derived from 4-Aminoantipyrien Derivatives, Microbiology 2009; 37, 141-146.
9. Mishchenco, A.V. Lukov V.V. and Popov, L.D. Synthesis and Physico-Chemical Study of Complexation of Glyoxylic Acid Aroylhydrazones with Cu(II) in Solution and Solid Phase, Journal of Coordination Chemistry 2011; 64,1963-1976. http://dx.doi.org/10. 1080/ 00958972.2011.585640
10. Kramer, D.N., Klein, N. and Baselice, R.A. Quantitative Determination of Glyoxylic Acid. Analytical Chemistry, 1999; 31, 250-252. http://dx.doi.org/10.1021/ac60146a028
11. Sokol, H.A. (1977) Determination of Pyruvic and Glyoxylic Acids in the Presence of Acetaldehyde, Analytica Chimica Acta 1977;89, 407-408. **Error! Hyperlink reference not valid.** (01)84741-3

12. Tharmaraj, P., Kodimunthiri, D., Sheela, C.D. and Shanmugapriya, C.S. (2009) Synthesis, Spectral Studies and Antibacterial Activity of Cu(II), Co(II) and Ni(II) Complexes of 1-(2-Hydroxyphenyl)-3-phenyl-2-propen-1-one)N2-[(3,5-dimethyl-1H-pyrazol-1-yl)methyl] Hydrazone, Journal of the Serbian Chemical Society, 2009; **74**, 927-938. http://dx.doi.org/10.2298/JSC0909927T.
13. N. Revathi, M. Sankarganesh, J. Rajesh, J.D. Raja, Biologically active Cu(II), Co(II), Ni(II)and Zn(II) complexes of pyrimidine derivative Schiff base: antioxidant, antibacterial and in vitro DNA binding, anti-cancer studies, J. Fluoresc, 2017, http:// dx.doi.org/10.1007/s10895-017-2118-y.
14. Anupama, B., Padmaja, M. and Kumari, C.G. , Synthesis, Characterization, Biological Activity and DNA Binding Studies of Metal Complexes with 4-Aminoantipyrine Schiff Base Ligand. E-Journal of Chemistry2012; 9, 389-400. http://dx.doi.org/10.1155/ 2012/291850
15. Raman, N., Sobha, S. and Selvaganapathy, M. (2012) Probing the DNA Binding Mode of Transition Metal Based Biologically Active Compounds: Validation by Spectroscopic Methods, International Journal of Pharma and Bio Sciences2012; 3, 251-268.
16. Manjula, B. and Antony, S.A. (2013) Arsenic Induced Biochemical Changes in Pernaviridisas Potential Biomarkers in Metal Pollution, Asian Journal of Biochemical and Pharmaceutical Research 2013; 3, 168-178.
17. Wang, X.Y., Wang, Z.M. and Gao, S. (2008) Constructing Magnetic Molecular Solids by Employing Three-Atom Ligands as Bridges. Chemical Communications, 2008, 281-294. http://dx.doi.org/10.1039/B708122G
18. Ju, Z.F., Yao, Q.X., Wu, W. and Zhang, I. (2008) Strong Electron-Accepting Methyl ViologenDication Confined in Magnetic Hosts: Synthesis, Structural, Characterization, Change-Transfer and Magnetic Properties, of [(MV)2[Ni-(SCN)5]. Cl.2H2O]n and [(MV)[M(N3)2 (SCN)2]] (M=Mn, Co). Dalton Transactions, 355-362. http://dx.doi.org/10.1039/B710628A
19. L. K. Abdul Karem, F. H. Ganim and R. K. Rahem Al-Shemary (2018) Synthesis, Characterization, Structural, Thermal, POM Studies, Antimicrobial and DNA Cleavage Activity of a New Schiff Base-Azo Ligand and Its Complexation with Selected Metal Ions. Biochem.Cell. Arch. 18(1), 1437-1448
20. Belaid, S., Landreau, A., Djebbar, S., Benali-Baitich, O., Bouet, G. and Bouchara, J. (2008) Synthesis, Characterization and Antifungal Activity of a Series of Manganese(II) and Cupper(II) Complexes with Ligands Derived from Reduced N,N-O- phenylenebis(salicylideneimine). Journal of Inorganic Biochemistry, 102, 63- 69.http://dx.doi.org/10.1016/j.jinorgbio.2007.07.001
21. El-Asmy, A.A., Al-Ansi, T.Y. and Shaiba, Y.M. (1989) Chelated Complexes of Cadmium(II), Cobalt(II), Copper(II),Mercury(II), Nickel(II), Uranyl(II) and Zinc(II) with Benzilbis(4-phenylthiosemicarbazone).Transition Metal Chemistry,14,446-452. http://dx.doi.org/10.1007/BF01092587.

22. S.M. Kumar, M.P. Kesavan, G.G.V. Kumar, M. Sankarganesh, G. Chakkaravarthi, G. Rajagopal, J. Rajesh, New heteroleptic Zn(II) complexes of thiosemicarbazone and diimine Co- Ligands: structural analysis and their biological impacts, J. Mol. Struct. 1153 (2018) 1– 11.
23. W. A Jaafar., S. M. Fezea and R. K. Rahem Al- Shemary (2018)Employing the Physicochemical, Spectroscopy, Antimicrobial and Antifungal Efficacy Studies of P- Hydroxy Acetophenone Based Azo Schiff Base Complexes, J. of Global Pharma Technology, 10(06):503-512
24. N. Revathi, M. Sankarganesh, J. Rajesh, J.D. Raja, (2017)Biologically active Cu(II), Co(II), Ni(II)and Zn(II) complexes of pyrimidine derivative Schi ff base: antioxidant, antibacterial and in vitro DNA binding, anti-cancer studies, J. Fluoresc., http:// dx.doi.org/10.1007/s10895- 017-2118-y.
25. M. Sankarganesh, P.A. Jose, J.D. Raja, M.P. Kesavan, M. Vadivel, J. Rajesh, R. Jeyamurugan, R.S. Kumar, S. Karthikeyan, (2017)New pyrimidine based ligand capped gold and platinum nanoparticles: synthesis, characterization, antimicrobial, antioxidant, DNA interaction and in vitro anti-cancer activities, J. Photobiol. B Biol. 176 44–53.
26. R. K Al-Shemary, W.A. Jaafar, and A.N Niseaf. Structure, diagnosis, and in the Vitro Antimicrobial evaluation of 2-amino pyridine-derived Ligand Schiff base and its complexes with Cu (II), Hg (II), Ni (II), Mn (II) and Co (II), Rese. J. of Pharma, Biolog.and Chem. Sci (RJPBCS),, June ,2017, 8(3), 14-183
27. R.K. Gupta, A. Kumar, R.P. Paitandi, R.P. Singh, S. Mukhopadhyay, S.P. Verma, P. Das,
28. D.S. Pandey, Heteroleptic arene Ru(II) dipyrrinato complexes: DNA, protein binding and anti-cancer activity against ACHN cancer cell line, Dalton Trans. 45 (2016) 7163–7177